

Structural, elastic, and electronic properties of deformed carbon nanotubes under uniaxial strainA. Pullen,¹ G. L. Zhao,^{1,*} D. Bagayoko,¹ and L. Yang²¹*Department of Physics, Southern University and A & M College, Baton Rouge, Louisiana 70813, USA*²*Eloret, NASA Ames Research Center, MS230-3, Moffett Field, California 94035, USA*

(Received 7 May 2004; revised manuscript received 20 January 2005; published 25 May 2005)

We report structural, elastic, and electronic properties of selected, deformed, single-wall carbon nanotubes under uniaxial strain. We utilized a generalized gradient approximation potential of density functional theory and the linear combination of atomic orbital formalism. We discuss bond-lengths, tubule radii, and the band gaps as functions of tension and compression strain for carbon nanotubes (10, 0), (8, 4), and (10, 10) which have chiral angles of 0, 19.1, and 30 deg relative to the zigzag direction. We also calculated the Young's modulus and the in-plane stiffness for each of these three nanotubes as representatives of zigzag, chiral, and armchair nanotubes, respectively. We found that these carbon nanotubes have unique structural properties consisting of a strong tendency to retain their tubule radii under large tension and compression strains.

DOI: 10.1103/PhysRevB.71.205410

PACS number(s): 73.22.-f, 61.46.+w

Single-wall carbon nanotubes (SWCNTs) can be viewed as rolled-up graphene sheets that have a diameter at the order of 1 nm. They have properties such as high current density, high elasticity, and stiffness unparalleled by other materials. Their potential applications range from that in building skyscrapers and elevator cables to the ones in very tiny electrical circuits and machines.¹ These materials, however, are too small for many conventional measurements. This situation underscores the possible importance of theoretical studies, including the one reported here that focuses on structural, elastic, and electronic properties of selected single-wall carbon nanotubes under uniaxial strain.

In the last several years, tight-binding calculations have been extensively used to study the structural and electronic structure of carbon nanotubes.²⁻⁶ Tight-binding approximations based on the symmetry of the honeycomb lattice of graphite predicted that SWCNTs could be semiconducting or metallic depending on their chirality (n, m). The tight-binding model has been able to provide good estimates of the basic electronic structure of SWCNTs. However, curvature-related effects and the hybridization of different electronic states of graphite could lead to structural and electronic properties that are substantially different from the result of tight-binding calculations. Zigzag ($n, 0$) (where n is a multiple of 3) SWCNTs which were predicted to be metallic from tight-binding calculations were found to have small energy gaps.⁷ Several theoretical groups have studied the elastic properties of carbon nanotubes. Their approaches include simulations with realistic many-body potentials,⁸ the empirical force-constant method,⁹ tight-binding formalisms,^{6,10} pseudopotential calculations with local density approximation potentials,¹¹ and Born's perturbation technique within a lattice dynamics model.¹²

The aim of this work is therefore to study the aforementioned properties of SWCNTs, utilizing *ab initio* quantum computations. We specifically report on structural, elastic, and electronic properties of SWCNTs under uniaxial strain. Recent tight-binding calculations have led to values of bond lengths and radii, band gaps, and Fermi levels as functions of strain.⁶ The dependence of tight-binding results upon the se-

lected parameters partly suggests the present work that employs an *ab initio* approach.

Three main features characterize our first-principles computational method. The first of these features is the choice of the potential. We utilized the generalized gradient approximation (GGA) potential of Perdew and Wang.¹³ This density functional¹⁴⁻¹⁶ potential goes beyond the local density approximation (LDA). We also performed LDA calculations for carbon nanotube (10, 0). The second feature of our method stems from employing the linear combination of atomic orbital (LCAO). The third and distinctive feature of our work resides in our use of optimal basis sets as per the Bagayoko, Zhao, and Williams (BZW) procedure.¹⁷⁻²⁰ As explained elsewhere, this procedure avoids a basis set and variational effect inherently associated with variational calculations that employ a basis set and leads to the calculated band gaps in very good agreement with experiments.¹⁷⁻²⁰ With the above method, we solved the Kohn-Sham^{14,15} equation self-consistently. Self-consistency was followed by the calculations of the total energies. Details of these steps, including the Kohn-Sham equation and the expression for the total energy, are fully described in the literature.¹⁴⁻²⁰

In the LCAO method, we expanded the electronic eigenfunction Ψ_{ki} of the many-atom system as a linear combination of atomic wave functions.¹⁷ These input functions result from *ab initio* calculations for atomic species that are present in the system. For the calculations, the C(1s) state was used as the core state. For the (10, 0) and the (8, 4) tubes, the C(2s2p) states were used as filled and partially filled valence states. The C(3s3p) orbitals were the unfilled electron states that were used to augment the basis set for the calculations. For the (10, 10) tube, the C(2s2p) states were used as filled and partially filled valence states and the C(3s) as the unfilled state. The empty C(3p) state was dropped, in the case of (10, 10), due to convergence difficulties.

Uniaxial strain was simulated by linearly scaling the atom positions along the tube axis in the carbon nanotube. To find how the tube radius changes with uniaxial strain, after the tube axis was scaled, the radius was identified from the total energy minimization procedure. Namely, for a given nano-

TABLE I. Unstrained bond lengths (a_0 , b_0 , and c_0) in carbon nanotubes (10,0), (8,4), and (10,10). L_0 is the length of the unit cell; r_0 is the tube radius; and N is the number of atoms per unit cell.

	(10,0)	(8,4)	(10,10)
a_0 (Å)	1.416	1.414	1.420
b_0 (Å)	1.416	1.419	1.420
c_0 (Å)	1.420	1.420	1.418
r_0 (Å)	3.915	4.143	6.781
L_0 (Å)	4.26	11.27	2.46
N	40	112	40

tube and a given compression or tensile strain, the total energy was obtained as a function of the tube radius. The equilibrium radius, i.e., the stable one, was the one corresponding to the minimum of the total energy. This process was repeated for each strain to obtain the radius of a tubule as a function of compression or tensile strain. Similarly, the calculated bond lengths, band gap, and Fermi energies, for a given nanotube and a given strain, are the one corresponding to the minimum of the total energies.

The Young's modulus for each SWCNT was calculated by fitting the total energy/unit cell for each strain ϵ_{zz} to the equation

$$E = \left[\frac{1}{2} \pi r^2 z Y \right] \epsilon_{zz}^2, \quad (1)$$

where Y is the Young's modulus, z is the unit cell length, and r is the outer radius of the nanotube. Equation (1) was derived using the assumption that the nanotube was a perfect cylinder.²¹ The standard radii tabulated for the nanotubes are for circumferences through the centers of the outer atoms. The outer radius includes such a standard radius plus the radius of the carbon atom (0.71 Å). We also calculated the in-plane stiffness C , which is an alternative measure of the mechanical characteristic of nanotubes that is defined as²²

$$C = \frac{1}{S} \frac{\partial^2 E}{\partial \epsilon_{zz}^2}, \quad (2)$$

where S is the surface area of the nanotube.

Table I displays the unstrained bond lengths and other characteristics of the tubules under study. In a graphene sheet, the lengths of the a , b , and c bonds are equal. In unstrained nanotubes, which are rolled graphene sheets, the three bonds are generally different. For the SWCNT (10, 0), the c bond along the axis is greater than the a and b bonds along the circumference ($a=b < c$). For the SWCNT (10, 10), the c bond along the circumference is shorter than the a and b bonds along the axis ($a=b > c$). In the case of the SWCNT (8, 4), the a bond closest to the circumference is less than the c bond closest to the axis, i.e., $a < b < c$. The bond lengths and radii as functions of the compression or tensile strain are displayed in Fig. 1 for the (10, 0) and Fig. 2 for the (8, 4). The calculated results for (10, 10) are very similar to those of (10, 0) and (8, 4) and are not presented in a separate figure, due to the page limitation of this brief

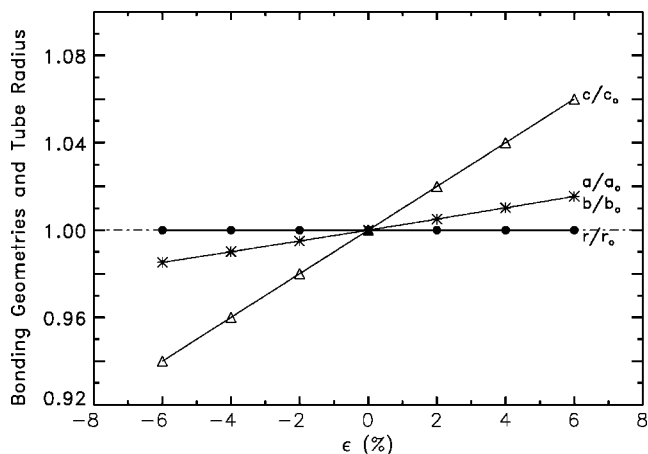


FIG. 1. Bond lengths and tube radius as functions of compression and tension strain ϵ for (10,0) nanotube. Each length is scaled to its unstrained length.

report. As per Figs. 1 and 2, the calculated and normalized lengths (i.e., a/a_0 , b/b_0 , or c/c_0) of bonds with a component along the axis decrease or increase linearly with compression or tensile strain, respectively. These variations are quantified with the slopes m provided in Table II.

A special feature of the calculated properties of the carbon nanotubes was that the radii of the nanotubes do not change under a substantially large uniaxial strain, from -6% to $+6\%$. The Poisson's ratio, which is the ratio of the transverse contracting strain to the longitudinal elongational strain, is nearly zero for these carbon nanotubes. This behavior is drastically different from that of macroscopic materials and it disagrees with results of tight-bonding calculations and other mechanics simulations.^{6,23} One possible explanation is that the bonds along the circumference, partly strengthened by curvature effects, are not significantly affected by uniaxial strains orthogonal to them (i.e., along the axis). We also repeated the studies using *ab initio* LDA calculations for SWCNT (10, 0). The total energy minimization of the LDA calculations for (10, 0) found the bond length at 1.402 Å for

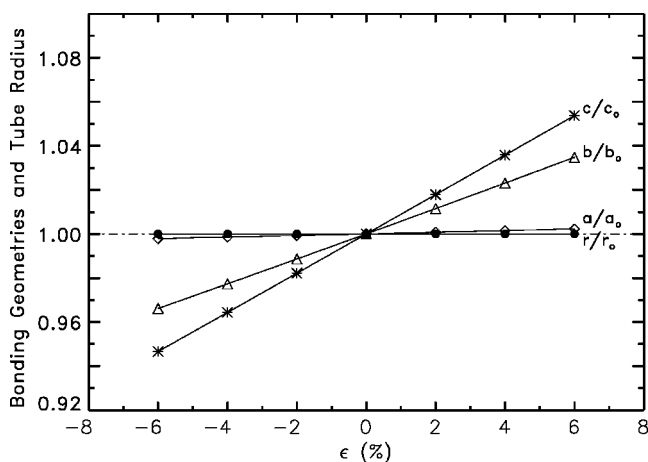


FIG. 2. Bond lengths and tube radius as functions of tension strain and compression strain ϵ for (8,4) nanotube. Each length is scaled to its unstrained length.

TABLE II. Coefficients m of linear variation of normalized bond lengths with compression (negative) and tensile (positive) strain (i.e., ϵ expressed as -0.04 and $+0.06$ for 4% and 6% compression and tensile strain, respectively). $\Delta l/l_0 = m\epsilon$, where l is the a , b , or c bond length. The Young's modulus Y is in TPa. The in-plane stiffness C is in J/m^2 .

Nanotubes	m for bond a	m for bond b	m for bond c	Y (TPa)	C (J/m^2)
(10,0)	0.252	0.252	1.000	1.47	340
(8,4)	0.036	0.572	0.893	1.10	267
(10,10)	0.746	0.746	0 ^a	0.726	272

^aBond c , for (10,10), is along the circumference of the tube.

a_0 and b_0 and 1.406 \AA for c_0 , that is about 1% smaller than the results of the *ab initio* GGA calculations. The *ab initio* LDA calculations for SWCNT (10, 0) also found that the radii of the nanotube did not change under a substantially large uniaxial strain. Among the previous *ab initio* calculations of the elastic properties of carbon nanotubes, Sanchez-Portal *et al.* utilized a minimal basis set of one s and three p orbitals per carbon atom and performed LDA calculations.²⁴ In their calculations, they used pseudoatomic orbitals.²⁴ Van Lier *et al.* utilized *ab initio* Hartree-Fock 6-31G method and closed nanotube models in their simulations.²⁵ Sanchez-Portal *et al.*²⁴ and Van Lier *et al.*²⁵ reported relatively small values (from 0.14 to 0.19) of the Poisson ratio for their calculated carbon nanotubes, which also indicated the diameter rigidity of the carbon nanotubes. These previous *ab initio* calculations utilized different computational methods, such as a minimal basis set and the Hartree-Fock method, and their results are slightly different from ours. As demonstrated in one of our previous publications,³⁰ the use of a minimal basis set may not be sufficient to obtain a highly accurate solution of the calculated electronic structure of the carbon nanotubes, which could explain in part the difference between our results and those of Sanchez-Portal *et al.* The fundamental differences between the Hartree-Fock method and density functional methods, i.e., the inclusion of the electronic correlation effects in the latter, partly explain the difference between our results and those of Van Lier *et al.* In our *ab initio* calculations, we utilized extended atomic basis sets and performed both GGA and LDA computations.

The calculated Young's moduli Y (in TPa) for the tubes are shown in Table II. We recall that the radius included in the formula for the Young's modulus is from the center of the tube to the outer circumference. This value of the radius led to Young's moduli close to the experimentally found value of approximately 1 TPa.⁹ The (10, 0) and (10, 10) tubes have the highest and lowest Young's moduli, respectively. This trend is expected due to the bond geometry of the tubes according to chirality. All three bonds in the (10, 0) tube have a significant component parallel to the axis along which strain is applied. In the case of (10, 0), the c bond is entirely along the axis. In contrast, one of the bonds of the (10, 10) tube is entirely along the circumference; it is not expected to oppose any resistance neither to compression nor to tensile strain. For this reason, nanotube (10, 10) is intuitively the

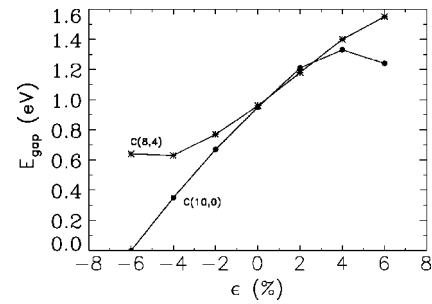


FIG. 3. Band gaps of indicated carbon nanotubes as functions of compression and tensile strain.

easiest to stretch or to compress, as confirmed by our results in Table II.

We also calculated the in-plane stiffness C for the carbon nanotubes. It is 340, 267, and 272 J/m^2 for (10, 0), (8, 4), and (10, 10), respectively. The in-plane stiffness of these nanotubes exhibited a dependence on their chirality, when the nanotubes are strained along the tube axis (z -direction). Xiao and Liao reported an average in-plane stiffness C of 328 J/m^2 for graphene, using the second-generation Brenner potential in their simulation of carbon nanotubes.²²

The calculated electronic properties for the unstrained nanotubes basically reproduced the results of Zhao *et al.*²⁰ for (10, 0) and (8, 4), using the optimal basis sets of the BZW method, which gave converged results for the calculated electronic structure that included the occupied electron states as well as the unoccupied ones near the Fermi level. These tubes were found to be semiconductors. These authors provided plots of the band structures of these tubes.²⁰ The electron energy bands of carbon nanotube (10, 10) present a semimetallic property as reported in previous publications. Figure 3 shows the nonlinear variation of band gaps of (10, 0) and (8, 4) with strain. For both nanotubes, the band gap decreases with compression strain and increases with tensile strain, for strain values smaller than or equal to 4%. While the band gap for (8, 4) reaches a minimum for a compression strain of 4%, that for (10, 0) exhibits a maximum for a tensile strain of 4%. Our results for the variation of the band gap with strain qualitatively agree with the findings from tight binding²¹ but are quantitatively different,⁶ particularly in the magnitudes of the band gaps. As apparent in Fig. 3, our results indicate that nanotube (10, 0) become metallic at 6% compression strain. It was noticed that the carbon nanotubes may collapse for large strains,^{32,33} a process that we cannot simulate at present using the *ab initio* quantum calculations, because the required computations are beyond our current computation capability. Therefore, the obtained band gaps for large strains may be a theoretical simulation. *A priori*, the general behavior of these band gaps with strain, particularly from values below 4%, is expected on the basis of the increase or decrease of the overlap between atomic sites, for compression or tensile strains, respectively. The consequent broadening or flattening of the bands, respectively, affects the gaps.

A discussion of our results for the elastic properties is partly limited by the dearth of experimental data and by the rather large uncertainty associated with currently available

ones. Indeed, Treacy *et al.*²⁶ and Wong and coworkers²⁷ reported average Young's moduli of 1.8 and 1.28 TPa with respective uncertainties of 1.4 and 0.59 TPa. Given these large error margins, the claimed agreement between our results and experimental ones may not have much significance. A comparison with previous theoretical studies is hampered by the differences in the expressions of the Young's modulus for carbon nanotubes as explained by Hernández and coworkers.¹⁰ These authors found 1.22 and 1.24 TPa for the Young's moduli of (10, 0) and (10, 10) respectively. The tight-binding work of these authors, as per their Fig. 3, led to about the same modulus for ($n, 0$) and (n, n) single-walled carbon nanotubes for diameters between 0.75 and 2 nm. This finding is qualitatively different from ours. Lu⁹ also found, using the empirical force-constant model, values of 0.975 and 0.972 TPa for (10, 0) and (10, 10), respectively. Our results are clearly different for the three nanotubes under consideration. Our results of 1.47 and 0.726 TPa for nanotubes (10, 0) and (10, 10), respectively, qualitatively agree with the trend in the recent tight-binding work of Zhang *et al.*²⁸ who found the elastic limit of ($n, 0$) tubes to be about twice that of (n, n) tubes of comparable radius. Another indication of the possible correctness of our findings may reside in the case of graphite. Indeed, the Young's modulus of graphite along the c axis, 0.0365 TPa, is very different from the one in the basal plane, 1.02 TPa.²⁹

Due to our utilization of the BZW method, our calculated band gaps are expectedly higher than other theoretical findings known to us. While Reich *et al.*³⁰ reported a gap of 0.8 eV for nanotube (8, 4), we found 0.96 eV. More importantly, our results clearly show that the variation of the band gap with strain is far from being linear. For nanotubes (10, 0) and (8, 4), the average increase of the band gap per tensile strain under 2% is 0.125 eV. This result is larger than a previously estimated maximum variation³¹ of 0.100 eV per percent strain, as is reportedly the case for bulk semiconductor.

In conclusion, this work reported the calculated structural, elastic, and electronic properties of selected, single-wall carbon nanotubes (10, 0), (8, 4), and (10, 10) under uniaxial

strain. The results of our *ab initio*, self-consistent, GGA-BZW calculations agreed qualitatively with some findings of the tight binding approach and quantitatively disagreed with them. We found that the radii of these nanotubes do not change under uniaxial strain, up to 6%. We quantified the linear variation of bond lengths with compression and tensile strain and showed the change of the band gap with strain, for semiconducting nanotubes, to be essentially nonlinear. Measurements of elastic limits for ($n, 0$) and (n, n) nanotubes and of the Young's moduli and the in-plane stiffness for graphite qualitatively agree with the trends in our calculated results for the selected single-walled carbon nanotubes.

Recently, we received two preprints regarding the experimental work by S. B. Cronin *et al.* at Harvard University and the Massachusetts Institute of Technology on measurements of uniaxial strain in single-wall carbon nanotubes, utilizing resonance Raman spectra of atomic-force microscope modified SWCNTs. This work entailed bending the nanotubes while holding the ends fixed. Two important comments should be made about this finding. The first one consists of the fact that our calculations did not include a determination of whether or not the nanotubes actually conserve their symmetrical geometry under strain as high as 6%. Cronin *et al.*³² reported cases where carbon nanotubes broke under strains greater than 1.65%. The second comment stems from an indication, from the work of Cronin *et al.*,^{32,33} that the radii of semiconducting SWCNTs do not change under strains between 0.06 and 1.65%. The constancy of the radial breathing mode (RBM) frequency (ω_{RBM}) lead to this conclusion,^{32,33} given that the tube diameter $d_t = 248/\omega_{\text{RBM}}$.

ACKNOWLEDGMENTS

This work was funded in part by the National Aeronautics and Space Administration (NASA Award No. NCC 2-1344), the Department of the Navy, Office of Naval Research (ONR, Awards No. N00014-05-1-0009 and No. N00014-04-0587), and the National Science Foundation (NSF Award No. HRD-0000272).

*Corresponding author. Email address: zhao@grant.phys.subr.edu
¹M. Wilson, K. Kannangara, G. Smith, M. Simmons, and B. Rague, *Nanotechnology: Basic Science and Emerging Technologies* (Chapman and Hall, Boca Raton, 2002).
²C. T. White and J. Mintmire, *Nature* (London) **394**, 29 (1998).
³J. W. Mintmire and C. T. White, *Phys. Rev. Lett.* **81**, 2506 (1998).
⁴L. Yang, M. P. Anantram, J. Han, and J. P. Lu, *Phys. Rev. B* **60**, 13 874 (1999).
⁵L. Yang and J. Han, *Phys. Rev. Lett.* **85**, 154 (2000).
⁶L. Yang, J. Han, M. P. Anantram, and R. Jaffe, *Comput. Model. Eng. Sci.* **3**, 675 (2002).
⁷M. Ouyang, J. L. Huang, C. L. Cheung, and C. M. Lieber, *Science* **292**, 702 (2001).
⁸B. I. Yakobson, C. J. Brabec, and J. Bernholc, *Phys. Rev. Lett.* **76**, 2511 (1996).

⁹J. P. Lu, *Phys. Rev. Lett.* **79**, 1297 (1997).
¹⁰E. Hernández, C. Goze, P. Bernier, and A. Rubio, *Phys. Rev. Lett.* **80**, 4502 (1998).
¹¹D. Sanchez-Portal, E. Artacho, J. M. Soler, A. Rubio, and P. Ordejón, *Phys. Rev. B* **59**, 12 678 (1999).
¹²V. N. Popov, V. E. Van Doren, and M. Balkanski, *Phys. Rev. B* **61**, 3078 (2000).
¹³J. P. Perdew and W. Yue, *Phys. Rev. B* **33**, 8800 (1986); J. P. Perdew, *ibid.* **33**, 8822 (1986); J. P. Perdew and A. Zunger, *ibid.* **23**, 5048 (1981).
¹⁴P. Hohenberg and W. Kohn, *Phys. Rev.* **136**, B864 (1964).
¹⁵W. Kohn and L. J. Sham, *Phys. Rev.* **140**, A1133 (1965).
¹⁶J. Callaway and N. H. March, in *Solid State Physics*, Vol. 38, edited by H. Ehrenreich, D. Turnbull, and F. Seitz (Academic Press, New York, 1984), p. 135, and references therein.
¹⁷G. L. Zhao, D. Bagayoko, and T. D. Williams, *Phys. Rev. B* **60**,

- 1563 (1999).
- ¹⁸D. Bagayoko, G. L. Zhao, J. D. Fan, and J. T. Wang, *J. Phys.: Condens. Matter* **10**(25), 5645 (1998).
- ¹⁹D. Bagayoko and G. L. Zhao, *Int. J. Mod. Phys. B* **13**(29, 30 & 31), 3767 (1999).
- ²⁰G. L. Zhao, D. Bagayoko, and L. Yang, *Phys. Rev. B* **69**, 245416 (2004).
- ²¹M. Dresselhaus, G. Dresselhaus, and P. Ecklund, *Science of Fullerenes and Carbon Nanotubes* (Academic Press, San Diego, 1996); also see C. Kittel, *Introduction to Solid State Physics*, 7th ed. (Wiley, Brisbane, 1996).
- ²²T. Xiao and K. Liao, *Phys. Rev. B* **66**, 153407 (2002).
- ²³A. Sears and R. C. Batra, *Phys. Rev. B* **69**, 235406 (2004).
- ²⁴D. Sanchez-Portal, E. Artacho, J. M. Soler, A. Rubio, and P. Ordejón, *Phys. Rev. B* **59**, 12 678 (1999).
- ²⁵G. Van Lier, C. Van Alsenoy, V. Van Doren, and P. Geerlings, *Chem. Phys. Lett.* **326**, 181 (2000).
- ²⁶M. M. J. Treacy, T. W. Ebbesen, and J. M. Gibson, *Nature* (London) **381**, 678 (1996).
- ²⁷E. W. Wong, P. E. Sheehan, and C. M. Lieber, *Science* **277**, 1971 (1997).
- ²⁸Peihong Zhang, Paul E. Lammert, and Vincent H. Crespi, *Phys. Rev. Lett.* **81**, 5346 (1998).
- ²⁹O. L. Blakslee *et al.*, *J. Appl. Phys.* **41**, 3373 (1970); E. J. Seldin and C. W. Nezheda, *ibid.* **41**, 3389 (1970).
- ³⁰S. Reich, C. Thomsen, and P. Ordejón, *Phys. Rev. B* **65**, 155411 (2002).
- ³¹E. D. Minot, Yuval Yaish, Vera Sazonova, Ji-Yong Park, Markus Brink, and Paul L. McEuen, *Phys. Rev. Lett.* **90**(15), 156401 (2003).
- ³²S. B. Cronin, A. K. Swan, M. S. Unlu, B. B. Goldberg, M. S. Dresselhaus, and M. Tinkham, *Phys. Rev. Lett.* **93**, 167401 (2004).
- ³³S. B. Cronin, A. K. Swan, M. S. Unlu, B. B. Goldberg, M. S. Dresselhaus, and M. Tinkham (unpublished).